Journal of Photochemistry and Photobiology A: Chemistry 157 (2003) 55–63

Journal of Photochemistry and Photobiology A:Chemistry

www.elsevier.com/locate/jphotochem

Photoelectrocatalytic degradation of Remazol Brilliant Orange 3R on titanium dioxide thin-film electrodes

Maria Valnice B. Zanoni[1], Jeosadaque J. Sene[2], Marc A. Anderson*

Environmental Chemistry and Technology Program, University of Wisconsin-Madison, 660 N. Park Street, Madison, WI 53706, USA

Received 20 May 2002; received in revised form 15 August 2002; accepted 21 August 2002

Abstract

Degradation of reactive dye Remazol Brilliant Orange 3R (RBO) has been performed using photoeletrocatalysis. A biased potential is applied across a titanium dioxide thin-film photoelectrode illuminated by UV light. It is suggested that charges photogenerated at the electrode surface give rise to chlorine generation and powerful oxidants ($OH^{\bullet}$) that causes the dye solution to decolorize. Rate constants calculated from color decay versus time reveal a first-order reaction up to 5.0×10^{-5} mol l^{-1} in dye concentration. The best experimental conditions were found to be pH 6.0 and 1.0 mol l^{-1} NaCl when the photoelectrode was biased at +1 V (versus SCE). Almost complete mineralization of the dye content (70% TOC reduction) was achieved in a 3-h period using these conditions. Effects of other electrolytes, dye concentration and applied potentials also have been investigated and are discussed.

Keywords: Photoelectrocatalysis; Degradation of azo dye; TiO_2 thin-film electrode; Electrolyte effects

1. Introduction

Reactive dyes are a class of synthetic dyes extensively used in the textile industry due to their characteristic of fixation in the fibers. In addition to the chromophore group, this kind of dye also exhibits a reactive group, which binds to the textile fibers through covalent bonds [1]. The dyeing process consists of two main steps: first, the fabric is immersed in a dyeing bath; and second, the dye in excess, not fixed onto the fabric, is removed by washing steps. The major environmental problem associated with the use of these reactive dyes is due to their inefficient fixation to the fibers. This is caused by the fact that commercial dyes are highly impure with the reactive group easily inactivated due to hydrolysis with –OH from the dye bath [2]. Therefore, significant losses (12–20% of the annual dye production) occur during the manufacture and processing with dyes being discharged as effluents into publicly owned water treatment plants. The variety of physical–chemical properties of each class of dyes and the introduction of several other chemicals during the dyeing process such as dispersing agents, salts and many others organics make the wastewater treatment a complicated process. Effluents from these wastewater treatments are processed into sludge cakes and deposited in landfills [3,4] resulting in further long-range environmental risk from these partially oxidized dyes.

Over the past few years, alternative methods [5–9] for dye treatment have been investigated, including chemical oxidation with reagents such as: ozone, hydrogen peroxide, ozone/UV, hydrogen peroxide/UV and Fenton's reagent (hydrogen peroxide + Fe(II). A photocatalytic method for the oxidation of dyes in wastewater using TiO_2 and UV or solar irradiation has also been investigated [10–12].

Relatively few studies for dye degradation [13–15] have been conducted using electrochemical oxidation. The electrolysis of dispersed dyes at Ti/Pt-Ir anode leads to 90% color removal and to the destruction of 40–79% of the chemical oxygen demand (COD) under acidic pH [13,14]. The use of Ti/RuO_2 as anode has also been reported to remove 92% of the COD in the treatment of a mixture of reactive acidic dyes [15].

An attractive process popularized in the past few years for degrading organic pollutants is the combination of electrochemical and photochemical technologies. Photoelectrocatalysis takes advantage of the heterogeneous photocatalytic process by applying a biased potential across a photoelectrode on which the catalyst is supported. This

* Corresponding author. Tel.: +1-608-262-2674; fax: +1-608-262-0454.
E-mail address: nanopor@facstaff.wisc.edu (M.A. Anderson).
[1] Present address: Instituto de Quimica—UNESP, Caixa Postal 355, 14800-901 Araraquara, SP, Brazil.
[2] Present address: Fundação Educacional de Barretos, Av. Prof. Roberto Frade Monte 389, CEP 14783-226, Barretos, SP, Brazil.

1010-6030/03/$ – see front matter
PII: S1010-6030(02)00320-9

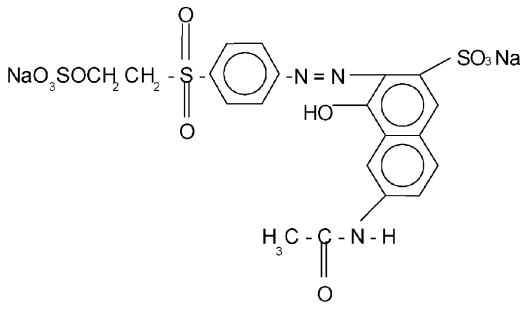

Fig. 1. Molecular structure of Remazol Brilliant Orange 3R (RBO).

configuration allows the more effective separation of photogenerated charges thereby increasing the lifetime of electron–hole pairs [16]. In spite of its real advantage, few studies have been conducted on the application of this new technology for the remediation of textile dyes [17–19].

Nanostructured semiconductor thin-film electrodes have been studied since their early introduction on supported ceramic membranes [20,21]. Titanium dioxide itself has been prepared by sol–gel chemistry techniques and coated on a variety of supports to produce thin-film photoelectrodes as reported previously [22,23]. These new electrodes have large internal surface areas. They are electrochemically stable and have a high efficiency for the decontaminating organic pollutants [24].

Azo dyes constitute a considerable part of the overall category of dyestuffs encountered in wastewater and probably have the least desirable consequence in terms of toxicity to aquatic biota and interference in natural photosynthetic phenomena. It is well known that the degradation of this kind of dye by usual metabolic routes leads to potentially hazardous aromatic amines [1]. Remazol Brilliant Orange 3R (RBO; Fig. 1) is a complex azo dye widely used in the textile industry despite the fact that it is not easily degraded by conventional methods.

In this work, we report on the photoelectrocatalytic degradation of RBO using titanium-supported titania photoelectrodes made by sol–gel techniques. The RBO degradation kinetics parameters have been evaluated through total organic carbon (TOC) removal and solution discoloration to assess the effectiveness of this method.

2. Experimental

2.1. Catalyst and photoelectrodes

Titanium(IV) isopropoxide (Aldrich) was used as a precursor for preparing TiO_2 colloidal suspensions. Typically, 20 ml of titanium isopropoxide was added to a nitric acid solution keeping the ratio $Ti/H^+/H_2O$ at 1:0.5:200. The resulting precipitate was continuously stirred until completely peptized to a stable colloidal suspension. This suspension was dialyzed against Milli-Q water to pH 3.5 by using a Micropore 3500 MW cutoff membrane [25]. Photoelectrode thin-films were cast onto titanium foil back contacts (0.05 or 0.5 mm thick, Goodfellow Cambridge Ltd.) following a sequence of dipping, drying and firing at 300 °C for 3 h. Further details concerning this procedure are available in the literature [22,23].

A detailed description of the characterization of these thin-film electrodes is presented elsewhere [26]. Briefly, however, the band gap energy was estimated by means of UV-Vis spectra recorded from thin films prepared by dip-coating square pieces of quartz slides (2 cm × 2 cm) in the sols. One layer of the nanocrystalline semiconducting material was estimated to be 100 nm thick in previous work [27]. The slides were fired at 350 °C for 3 h in order to be compared with the actual thin-film electrodes used in the photoelectrocatalytic experiments. The UV-Vis spectra were recorded using a blank slide as a reference. A blue shift of 0.19 eV in the band gap energy, compared to bulk titanium dioxide, is observed in the profile of the absorption spectrum due to quantum-size effect of the small particles in the sol. Accordingly, the TiO_2 prepared by the sol gel chemistry method presents an onset of absorption at 360 nm, giving a band gap energy of 3.44 eV for these thin-film electrodes.

2.2. Test cells

Photocurrent measurements and flat band potential determinations were carried out using a 30-ml single-compartment Teflon cell having a circular quartz window of 50-mm diameter. A circular opening in the cell opposite the quartz window allowed exposure of 4.5 cm^2 of the working electrode (TiO_2) to UV illumination. The platinum foil counter electrode (9.0 cm^2), having a circular opening of the same size as the light pathway, was placed just in front of the working electrode, 1 cm away. A saturated calomel electrode (SCE), used as a reference, was placed close to the working electrode through a bridge tube with a Vycor frit tip.

The photoelectrocatalytic degradation experiments were performed in a two-compartment reactor. A Nafion 117 membrane was used to separate both compartments while allowing electrolyte contact. The photoactive area of the anode (TiO_2) was 10 cm^2 and was illuminated by a 450 W Xe–Hg arc lamp (Oriel, model 6262) UV light source through a quartz circular window mounted in one of the sides of the cell. The compartment containing the platinum counter electrode of approximately the same area was not directly exposed to the UV illumination. The reference electrode was the same SCE mentioned above. A Princeton Applied Research (PAR) potentiostat model 6310 was used to bias the photoanode in the photoelectrocatalytic experiments and also to record the linear sweep voltammetry (LSV) plots for measuring photocurrents. All LSV measurements employed a voltage sweep of 10 $mV\,s^{-1}$.

All experiments employed the same UV light source. The irradiance at the working electrode surface was

50 mW cm^{-2}, as measured with an International Light Inc. model IL 1400A photometer.

2.3. Spectroscopy and organic carbon analysis

Absorption spectra in the ultraviolet and visible range were recorded with a Hewlett-Packard spectrophotometer, model HP 8452A in a 10 mm quartz cell. A total organic carbon analyzer (Shimadzu Instruments, model TOC 5000) was used to monitor organic carbon removal.

2.4. Eletrophoretic mobility measurements

The electrophoretic mobility of TiO_2 particles dispersed in 0.010 mol l^{-1} KNO_3 and containing 0.001 mol l^{-1} RBO dye was measured with a Zetasizer (Malvern Instruments, model 5000). Water was evaporated from TiO_2 aqueous suspensions producing a xerogel that was fired at 300 °C for 5 h. The solid was ground in an agate mortar and a 2.0 g l^{-1} suspension was prepared in KNO_3 solution. The pH was adjusted by adding appropriate amounts 0.1 mol l^{-1} HNO_3 or KOH under N_2 atmosphere. The samples were stored under N_2 atmosphere for 12 h at room temperature to allow the surface to equilibrate with the solution and the pH was rechecked just prior to mobility measurement.

3. Results and discussion

The remarkable synergistic effect of a biased photoanode on the photocatalytic process during the discoloration of a 5×10^{-5} mol l^{-1} RBO dye solution in 0.5 mol l^{-1} NaCl can be observed in Fig. 2. Fig. 2a shows the performance of the TiO_2 thin-film electrodes with respect to color removal evaluated as a fractional conversion (f) of the dye and plotted in a time-dependent scale. Three distinct conditions were investigated: (a) the photocatalytic treatment by using UV light without a bias potential; (b) the electrocatalytic treatment by biasing the electrode with +1 V (SCE) in dark conditions and (c) finally the photoelectrocatalytic treatment, i.e. using both UV light and 1.0 V (SCE) of bias potential. The fractional conversion is the ratio of dye concentration variation at time t (C_t) to the initial dye concentration (C_0) in solution at $t = 0$.

Concentration was determined by monitoring the absorbance of RBO dye at $\lambda = 492$ nm, from the UV-Vis absorption spectra as a function of time (shown in Fig. 2b). It can be seen that absorbance decreases as a function of time during photoelectrocatalysis. The RBO dye obeys Beer's law for concentrations up to 1.5×10^{-4} mol l^{-1}; $\varepsilon = 1.324 \times 10^4$ mol l^{-1} cm^{-1}. The results obtained (Fig. 2b) show that the photoelectrocatalytic approach promotes the decrease of all peaks of the chromophore in the dye molecule. Furthermore, fractional conversions indicate complete removal of color when 100 ml of the dye is photoelectrolyzed for 30 min at +1 V under UV illumination. On the other hand, only 16 and 9% of color removal was observed in the photocatalytic or electrocatalytic treatment, respectively. These results illustrate that dye degradation by photoelectrocatalytic procedures is more effective than the expected summation of electrochemical degradation and photocatalytic effects. Instead, a synergistic effect seems to play a major role in the final treatment. By applying a bias potential one significantly increases the efficiency of the photocatalytic activity of the Ti/TiO_2 electrode and thereby increases the reaction rate of dye oxidation.

In order to obtain more information about the photoelectrocatalytic process and to optimize the method for degrading RBO, we also investigated other parameters controlling this process such as nature of supporting electrolyte, the pH

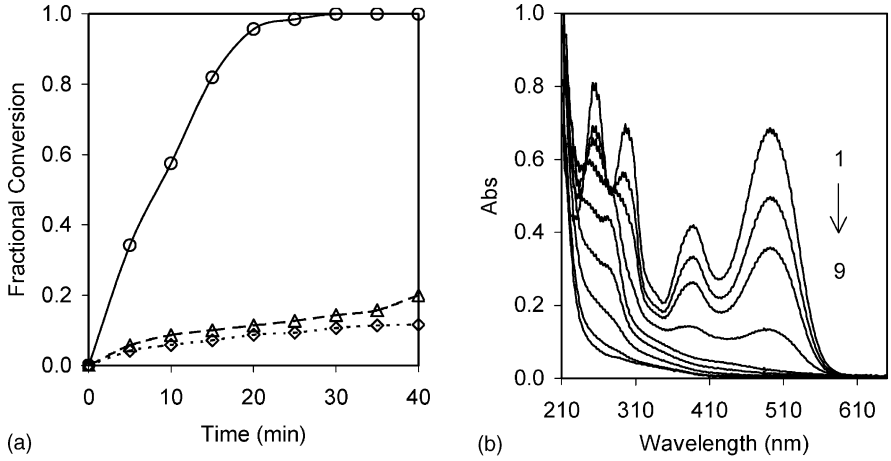

Fig. 2. (a) Comparison of reactive dye concentration reduction as a function of treatment time for: (◇) the photocatalytic process using UV light, (△) the electrocatalytic process applying $E = +1$ V and (○) the photoelectrocatalytic process with both UV light and $E = +1$ V. In all cases, dye concentration was 5×10^{-5} mol l^{-1} in 0.5 mol l^{-1} NaCl and pH 6.0. The anode was a Ti/TiO_2 thin-film electrode. (b) UV-Vis absorption spectra for 5×10^{-5} mol l^{-1} RBO dye in 0.5 mol l^{-1} NaCl at pH 6.0 before (Curve 1) and after photoelectrocatalytic degradation on the TiO_2 thin-film electrode biased at +1.0 V (vs. SCE) with the aliquots being removed each 5 min (Curves 2–9).

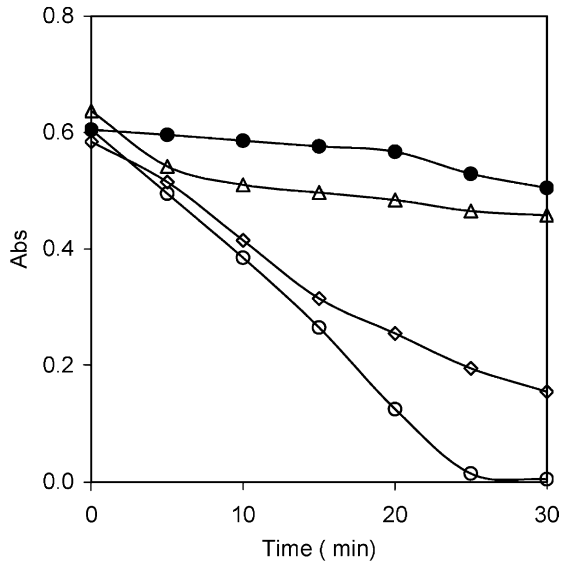

Fig. 3. Results from the photoelectrocatalytic oxidation of 5×10^{-5} mol l^{-1} RBO dye at pH 6.0 in 0.5 mol l^{-1} of: (○) NaCl, (◇) KNO_3, (△) $NaClO_4$ and (●) Na_2SO_4 using UV light and $E = +1$ V (vs. SCE).

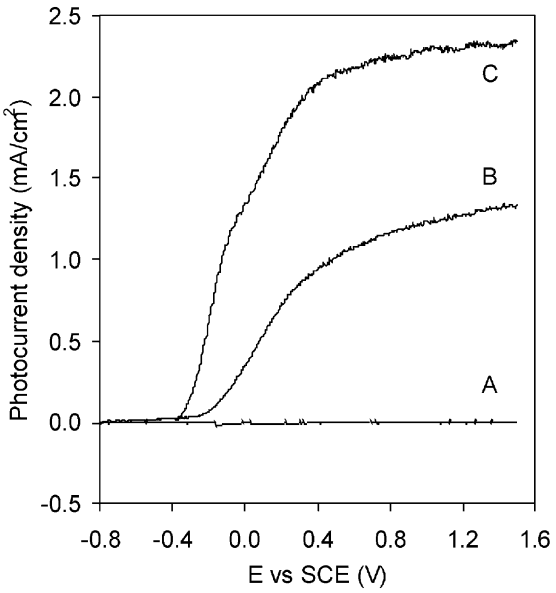

Fig. 4. Photocurrent–potential curves obtained for TiO_2 thin-film electrodes under dark conditions (Curve A) and for 0.5 mol l^{-1} Na_2SO_4 (Curve B) and 0.5 mol l^{-1} NaCl (Curve C) under UV illumination. Scan rate = 10 mV s^{-1}, pH 6.0.

of the solution, the applied voltage and the dye concentration.

3.1. Effect of supporting electrolyte

The influence of the type of electrolyte on the removal of color was investigated through experiments conducted with 5.7×10^{-5} mol l^{-1} RBO in 0.25 mol l^{-1} NaCl, $NaClO_4$, KNO_3 and Na_2SO_4. Dye absorbance was monitored during 30 min of photoelectrocatalytic degradation ($E = +1$ V, pH 6.0) and the degradation transients are presented in Fig. 3. The results obtained show that the selection of a supporting electrolyte for the complete removal of color is critical to the process. The degree in discoloration is 28 and 19% when $NaClO_4$ and Na_2SO_4 are used as electrolytes, respectively. On the other hand, KNO_3 promotes 75% of color removal after 30 min. This occurs due to photolytic reaction of NO_3^- under irradiation of $\lambda < 380$ nm by the overall reaction [24]:

$$NO_3^- + H_2O + h\nu \rightarrow NO_2^\bullet + OH^\bullet + OH^-$$

Therefore, the photocatalytic oxidation properties of NO_3^- also are likely for increasing the concentration of hydroxyl radicals and thereby increasing the discoloration rate of the dye. Nevertheless, in subsequent experiments we did not consider KNO_3 as a supporting electrolyte since the UV-Vis spectrum obtained after photocatalysis of the dye showed the occurrence of extra peaks in the UV region, suggesting other pathways for the photooxidation route or, alternatively, the corrosion of the coated catalyst. Most importantly, the highest discoloration rate is observed in chloride media, indicating that the mechanism of RBO degradation in NaCl solution may be different than that operating in the other supporting electrolytes.

Photocurrent–potential curves under dark conditions (Curve A) and under UV illumination, both in 0.5 mol l^{-1} Na_2SO_4 (Curve B) and NaCl (Curve C) are compared to each other in Fig. 4. According to the literature [16], by illuminating the semiconductor with light energy greater than that of the band gap, electron–hole pairs are generated at the electrode surface. A bias potential positive to the flat-band potential produces a bending of the conduction band causing a more effective charge separation and increases the photocurrent (I_{ph}) that begins to flow and likely promotes a better oxidative degradation process.

As expected, Fig. 4 shows that, under UV illumination, the TiO_2 photoelectrode gives rise to a photocurrent in Na_2SO_4 at -0.20 V, but in NaCl media the onset potential shifts to a less positive potential of -0.38 V, both at pH 6.0. In addition to this shift in potential, photocurrent in NaCl media was higher than in any other tested electrolyte.

It is well known [16,19,24] that the shape of the photocurrent voltammograms reflects the balance between the recombination of electron–hole pairs and substrate photooxidation. By applying an anodic bias potential to a working electrode we provide a potential gradient within the photocatalyst film to efficiently force the electrons to arrive at the counter electrode and leave photogenerated holes to react with H_2O/OH^- to give rise to $OH^\bullet$ radicals as shown by the global reaction that can be assigned using Eqs. (1)–(4).

Photoanode:

$$TiO_2 + h\nu \rightarrow TiO_2 - e_{cb}^- + TiO_2 - h_{vb}^+ \quad (1)$$

$$TiO_2 - h_{vb}^+ + H_2O_s \rightarrow TiO_2 - OH_s^\bullet + H^+ \quad (2)$$

$$TiO_2 - h_{vb}^+ + OH_s^- \rightarrow TiO_2 - OH_s^\bullet \quad (3)$$

Cathode (counter electrode):

$$2H_2O + 2e^- \rightarrow H_2 + 2OH^- \quad (4)$$

where the subscripts cb and vb denote conduction band and valence band of the photocatalyst and h^+ and e^- denotes photogenerated holes and electrons, respectively. The application of a positive potential higher than the flat-band potential on the Ti/TiO_2 electrode decreases the charge recombination process shown in Eq. (5), which is essential for promoting substrate degradation.

$$TiO_2 - e^-_{cb} + TiO_2 - h^+_{vb} \rightarrow \text{heat} \quad (5)$$

Therefore, at higher bias potentials the recombination rate (Eq. (5)) is minimized and the rate of the competitive reactions (Eqs. (2) and (3)) are increased as Eq. (4). Under these circumstances, it is possible to notice the concomitant increasing in the photocurrent density.

Nevertheless, in comparing Curves B and C in Fig. 4, one can notice that the nature of the electrolyte affects the photocurrent. The photocurrent intensity obtained for sulphate solutions corresponds simply to the contribution from the injection of electrons in the conduction band and hole transfer rate scavenged by OH^-. On the other hand, it is known that chloride ions are commonly electrochemically oxidized to chlorine at potentials around +1.3 V (versus Ag/AgCl) [28]. We therefore suspected that chloride ions might be oxidized at a less positive potential under photoelectrocatalytic conditions as denoted by Eq. (6):

$$TiO_2 - h^+_{vb} + Cl^-_s \rightarrow TiO_2 - Cl_s^\bullet \quad (6)$$

To confirm this hypothesis, photoelectrocatalytic studies of a 0.5 mol l^{-1} NaCl solution at pH 6.0 were conducted under UV illumination at $E = +1$ V. Aliquots were removed after 30 min of photoelectrocatalysis and analyzed using the standard colorimetric method based on the *N*,*N*-diethyl-*p*-phenylenediamine (DPD) indicator for free chlorine [29]. Results obtained showed that an average of 12.3 mg l^{-1} of chlorine gas is generated over the time of experiment. These experiments confirm that active chlorine can be produced at high concentrations on Ti/TiO_2 photoelectrodes.

In order to test the hypothesis that free chlorine acts as oxidative species in the degradation process, we compared photoelectrocatalysis with the chemical oxidation of 5.3×10^{-5} mol l^{-1} RBO by bubbling free chlorine into the test solution. Chlorine gas was generated by the direct reaction of $KMnO_4$ with concentrated HCl. Changes in the absorbance of the original dye were monitored during these experiments at various time intervals. Total color removal was obtained after adding a relatively high level of free chlorine. These results suggest that chlorine generation during the photoelectrocatalytic reaction may be one of the oxidizing species leading to the discoloration of the dye. Treatment of 5×10^{-5} mol l^{-1} RBO in NaCl at concentrations varying from 0.1 to 1.0 mol l^{-1} were carried out in order to obtain more information about the influence of

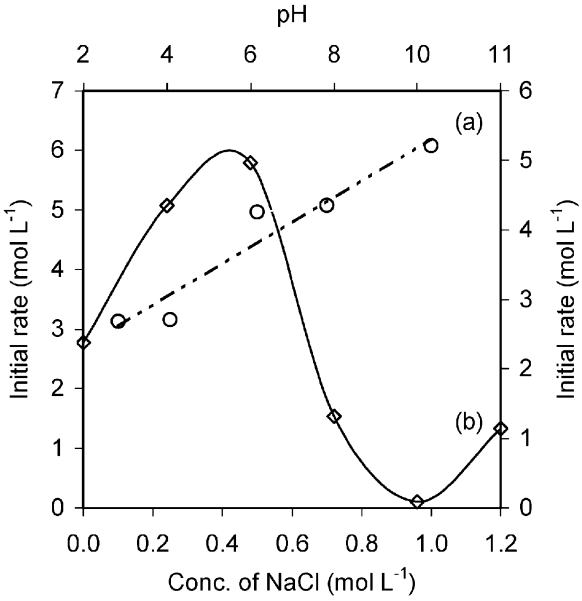

Fig. 5. Effect of NaCl concentration at pH 6.0 (Curve a) and pH variation in solutions 0.5 mol l^{-1} NaCl (Curve b), on the initial rate of photoelectrocatalytic oxidation of 5×10^{-5} mol l^{-1} RBO dye on a TiO_2 thin-film electrode biased at $E = +1$ V (vs. SCE).

NaCl on the dye discoloration. The dependence of the initial degradation rate evaluated from slopes of the curves obtained for dye consumption (mol l^{-1}) as function of time (s) at different NaCl concentration is presented in Fig. 5 (Curve a). Initial degradation rates linearly increase with the increase in the chloride concentration. This suggests that at initial dye concentrations of 5×10^{-5} mol l^{-1} color removal follows a first-order process with respect to Cl^- anions.

The dependence of photocurrent and dye discoloration rate on chloride concentration may be attributed to the improvement of Cl^- adsorption on the electrode surface under conditions of high concentrations of chloride [19]. At higher adsorption conditions, electron/holes generated at a steady rate or $OH^\bullet$ radicals are more easily transferred to the Cl^- ions improving the photocatalysis process due to the minimization of charge recombination.

From these data it is clear that the direct electrooxidation of RBO has a lower reaction rate on TiO_2 thin-film electrodes. However, the experimental conditions attained in the presence of Cl^- noticeably increase the efficiency of color removal. Although color removal is important, the major practical interest in using the photoelectrocatalytic method is the degree to which we mineralize the dye. In this context, experiments have been conducted by monitoring the TOC removal under the same operational conditions used for color removal.

The TOC results obtained for aliquots of 5×10^{-5} mol l^{-1} RBO in 0.50 mol l^{-1} of NaCl, $NaClO_4$, KNO_3 and Na_2SO_4 submitted to photoelectrocatalytic treatment during 30 min at a potential of +1 V, under UV illumination are presented

Table 1
Total organic carbon removal by photoelectrocatalytic oxidation of 5.0×10^{-5} mol l^{-1} RBO in 0.5 mol l^{-1} NaCl at pH 6.0 and $E = +1$ V (vs. SCE) on TiO_2 thin-film electrodes over a 30 min experiment

Influence of pH[a]		Influence of electrolyte[b]		Influence of potential[c]	
pH	TOC removal (%)	Eletrolyte (0.5 mol l^{-1})	TOC removal (%)	Potential (V)	TOC removal (%)
2	14.3	NaCl	28.4	+0.4	21.0
4	17.1	KNO_3	24.8	+0.6	25.9
6	28.4	$NaClO_4$	19.7	+0.8	29.7
8	22.5	Na_2SO_4	15.5	+1.0	36.3
10	27.0			+1.2	22.6
11	21.0				

[a] 0.5 mol l^{-1} NaCl, $E = +1$ V (vs. SCE).
[b] $E = +1$ V (vs. SCE), pH 6.0.
[c] 0.5 mol l^{-1} NaCl, pH 6.0.

in Table 1. Although color removal reaches 100% in NaCl electrolyte, the TOC removal is smaller than hoped but greater than values obtained for the other electrolytes. There are two main factors influencing the photodegradation of the dye. With the $NaClO_4$, KNO_3 and Na_2SO_4 salts, the photogenerated holes can react with OH^- or H_2O to form $OH^\bullet$ radicals (Eqs. (2) and (3)), which can oxidize the dye. However, we suspect that in chloride medium the photocatalytic activity is accentuated since Eq. (6) is also taking part in the process and is responsible for faster dye decomposition. For this reason, further photoelectrocatalytic experiments involving RBO degradation were investigated in 0.5 mol l^{-1} NaCl solutions.

3.2. Effect of pH

The influence of pH on the discoloration rate of RBO is presented in Fig. 5 (Curve b). Initial degradation rates are plotted as function of different pH values ($C_0 = 5 \times 10^{-5}$ mol l^{-1}, $E = +1$ V and 0.5 mol l^{-1} NaCl). It can be seen that the degradation rate is highest over the pH range 4–6 and decreases noticeably at higher pH.

TOC results monitored after the end of each experiment (30 min) are also presented in Table 1. Although the pH markedly affects the discoloration rate, a maximum TOC reduction of 28% was obtained at pH 6. These results show that color removal is to a great extent faster at acidic medium but mineralization could be preponderant at pH $\geq$ 6. In all further investigations pH 6.0 was selected as the optimum pH to investigate the dye degradation using chlorine medium, where mineralization and color removal are favorable.

Since the surface charge of the titanium dioxide electrode is influenced by the pH of the solution and by dissolved species, we have used electrophoresis to determine the changing in the isoelectric point of TiO_2 as caused by the presence of the RBO dye. Fig. 6 shows the results of measuring the zeta potential for suspended TiO_2 particles as function of the pH of the suspension. The pH of the isoelectric point for TiO_2 was found to be 5.0 in 0.01 mol l^{-1} KNO_3 in the absence of the dye. However, the addition of the RBO dye (0.06 mM) causes the isoelectric point of TiO_2 to move to pH 2.0 as Curve b in Fig. 6 shows. These results indicate that the adsorption of the RBO dye onto TiO_2 makes its surface more negatively charged, shifting the isoeletric point of TiO_2 three pH units backward compared with the pure electrolyte. Similar results have been found for the adsorption of phosphate anion onto TiO_2 [30]. Due to the fact that the RBO dye has a negative charge, the applied positive potential on the working electrode may increase its adsorption. At pH values higher than the isoelectric point, negative ions are repelled from the TiO_2 surface. In addition, by increasing the pH of the solution, the concentration of OH^- also increases, which is responsible for hydroxyl radical generation during the photocatalytic oxidation process. As a consequence, both the percentage of chlorine generation and the adsorption of the dye are diminished in conditions where the pH of the solution is higher than the pH of isoelectric point.

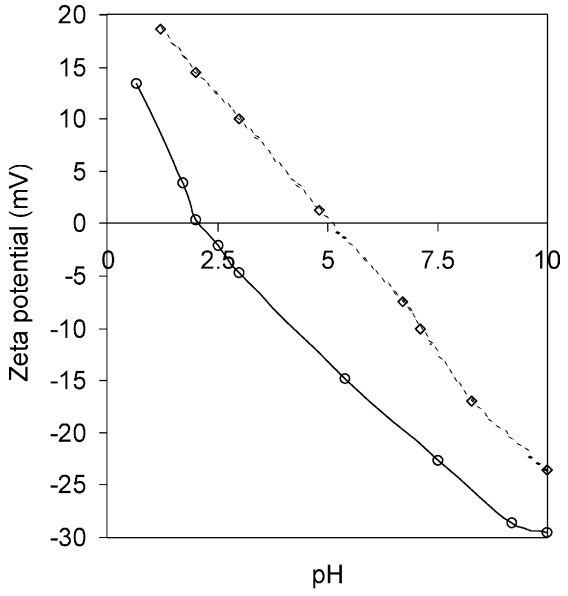

Fig. 6. Electrophoretic curves for TiO_2 nanoparticles suspended in 0.01 mol l^{-1} KNO_3 as a function of the pH of the suspension: (◇) no dye added and (○) with 0.06 mol l^{-1} RBO dye added.

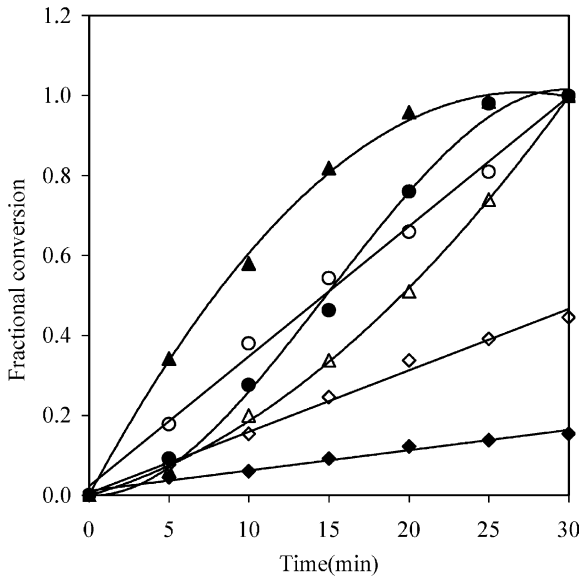

Fig. 7. Influence of the applied potential on color removal of 5×10^{-5} mol l^{-1} RBO dye in 0.5 mol l^{-1} NaCl at pH 6.0 by photoelectrocatalytic oxidation over a TiO_2 thin-film electrode: (◆) 0.2 V, (◇) 0.4 V, (△) 0.6 V, (●) 0.8 V, (▲) 1.0 V and (○) 1.2 V (vs. SCE).

3.3. Effect of applied potential

Experiments were conducted in 5×10^{-5} mol l^{-1} RBO using the best conditions defined previously to check for the importance of selecting the best potential for this process. Potentials ranged between +0.2 and +1.2 V and absorbance decay at 496 nm was monitored over 30 min of the experiment. Results are presented as fractional conversion (f) in Fig. 7. These results clearly demonstrate that the degradation rate increases as a function of applied potential up to $E = +1$ V. Further increases in potential lead to a slight reduction in degradation. TOC results obtained at the end of each experiment revealed analogous trends, as can be seen in Table 1.

As calculated from onset potential measurements, the flat-band potential for TiO_2 at pH 6.0 in 0.5 mol l^{-1} NaCl media is about −0.38 V. All of the applied potentials employed in this study are positive of this flatband potential. Therefore, there is always a potential gradient over the titania film, resulting in an electric field, which keeps photogenerated charges apart. These results suggest that adsorption of the RBO dye is enhanced and/or the generation and separation of electron–hole pairs are accelerated under higher voltage conditions. As a result, the rate of recombination decreases, so as to increase the photocurrent as a function of the applied potential. Accordingly, more of the active oxidizing radical species are thereby formed at higher potential, which promotes faster dye decomposition. In all further experiments +1 V was chosen as best potential for investigating the degradation of the RBO dye.

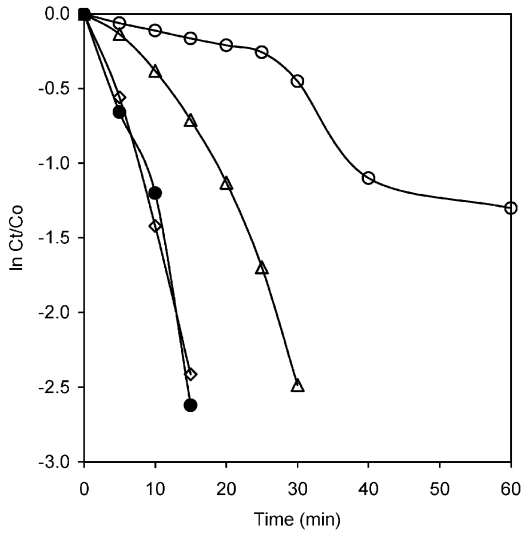

Fig. 8. Logarithm of normalized concentration of RBO as a function of: (◇) 1.5×10^{-5} mol l^{-1}, (●) 2.5×10^{-5} mol l^{-1}, (△) 5×10^{-5} mol l^{-1} and (○) 8×10^{-5} mol l^{-1} RBO dye in 0.5 mol l^{-1} NaCl pH 6.0 and electrode biased at $E = +1$ V (vs. SCE).

3.4. Effect of dye concentration

The influence of the initial concentration of RBO on the photoelectrocatalytic dye decomposition was investigated by keeping constant all previously optimized parameters in order to obtain the best performance of the photoelectrode. Dye concentration ranged from 1×10^{-5} to 8×10^{-5} mol l^{-1}. The photoelectrocatalytic decomposition of the RBO in 0.5 mol l^{-1} NaCl at $E = +1$ V was followed by measuring the absorbance decay at $\lambda = 496$ nm over 30 min. The decrease in concentration as a function of time was plotted as ln [A]t/[A] versus t and is shown in Fig. 8.

Clearly, there is a linear relationship up to 5.0×10^{-5} mol l^{-1} of the dye as function of the time of treatment, with a calculated slope of -0.162 s^{-1}, which is a typical behavior of a first-order reaction in dye consumption. Nevertheless, a deviation is observed at higher RBO concentration. As can be seen in Fig. 8, at the dye concentration of 8×10^{-5} mol l^{-1}, the degree of discoloration process in 0.5 mol l^{-1} NaCl is always lower than 77% even after 60 min of treatment. The decrease in dye degradation rate at higher initial RBO dye concentrations can be explained by the fact that at higher RBO dye concentrations the light intensity reaching the TiO_2 film surface is reduced due to the lower transparency of the solution. In addition, the formation of dye aggregates in solution usually begins at concentrations higher than 0.1 mM and the process is somehow influenced by NaCl concentration, as demonstrated in Fig. 9. This experiment was carried out both in 0.5 and 1.0 mol l^{-1} NaCl, under the same experimental conditions as in Fig. 8, and reveals that 100% of color removal is attained after 25 min of experiment when the concentration of NaCl is 1.0 mol l^{-1}, which suggests that the dye degradation depends on the ratio [NaCl]/[dye] in terms of concentration.

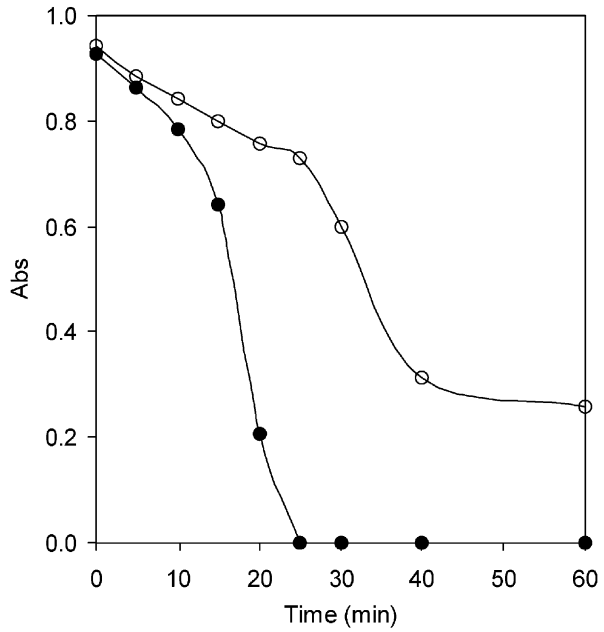

Fig. 9. Effect of concentration of NaCl on absorbance decay of 8.0×10^{-5} mol l^{-1} RBO dye at pH 6.0 as a function of time of photoelectrocatalytic oxidation over a TiO_2 thin-film electrode biased at $E = +1$ V (vs. SCE): (○) 0.5 mol l^{-1} NaCl and (●) 1.0 mol l^{-1} NaCl.

Lastly, we conducted a series of experiments over a 3-h period using 5×10^{-5} and 2×10^{-5} mol l^{-1} RBO in NaCl 1.0 mol l^{-1} with the photoanode biased at +1 V in order to further investigate the full potential of the photoelectrocatalytic approach. The overall results from TOC measurements are given in Fig. 10. Several repetitions of the methodology

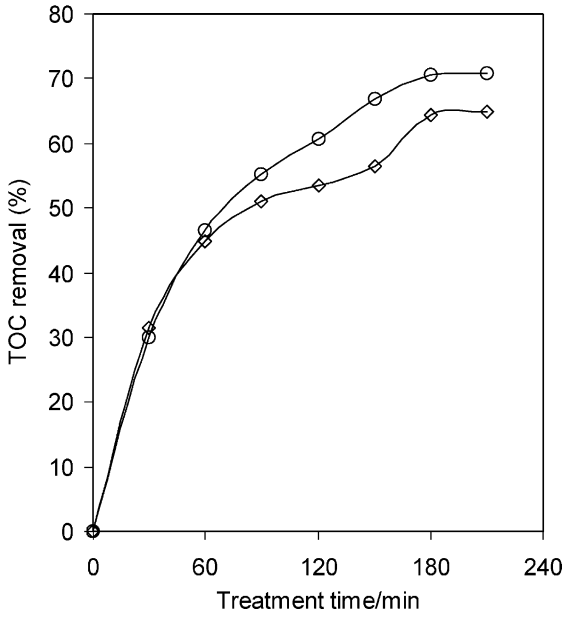

Fig. 10. Total organic carbon removal from (◇) 2.5×10^{-5} mol l^{-1} and (○) 5×10^{-5} mol l^{-1} RBO dye as a function of time during the photoelectrocatalytic treatment over a TiO_2 thin-film electrode biased at $E = +1$ V (vs. SCE). Both solutions in 0.5 mol l^{-1} NaCl pH 6.0.

demonstrated that a complete removal of color occurs after few minutes but longer times are needed to a more complete mineralization of the dye. We have obtained 70% of mineralization after 3 h of experiment using the best conditions of the method. Further experiments concerning reaction products and additional improvements to this process are now in progress.

4. Conclusions

This study demonstrates that a photoeletrocatalytic procedure leads to a fast and complete discoloration of RBO with a significant mineralization of the dye (70%) after 3 h of treatment. Although other studies have used NaCl as a supporting electrolyte in the photoelectrocatalytic oxidation of organic compounds, our results indicate that under certain biasing conditions on the Ti/TiO_2 photoelectrode the process may lead to active chlorine generation. While our process can easily decolorize textile wastes, the by-products of this process may or may not be acceptable to treatment plants. We are now analyzing these secondary products so as to ascertain their suitability for further treatment.

The best conditions for maximum photoelectrocatalytic degradation were found to be pH 6 at a potential of +1 V. The highest RBO degradation rate was found to occur in chloride solution, which in turn seems to account for generation of powerful oxidants such as $Cl_2^{\bullet}$, $Cl^{\bullet}$ and $OH^{\bullet}$ radicals that are directly responsible for fast dye degradation. Despite the fact that chlorine has been used extensively as a disinfectant for water purification systems, our method warrants further studies to clarify the dye degradation mechanism using chlorine generation since chlorinated compounds could result in this process.

Despite these uncertainties we believe that the use of TiO_2 thin-film photoelectrodes prepared by sol–gel methods has proven to be a powerful, efficient alternative to usual approaches applied to the discoloration and mineralization of the azo family of reactive dyes at low concentration. This is of importance because most of the wastewater treatments available until now for remediation of recalcitrant reactive dyes are in most cases based on phase transfer techniques.

Acknowledgements

Financial support from Brazilian funding agencies Capes, CNPq and Fapesp are gratefully acknowledged.

References

[1] H. Zollinger, Color Chemistry: Synthesis, Properties and Applications of Organic Dyes and Pigments, VCH Publisher, New York, 1987.
[2] R. Camp, P.E. Sturrock, Water Res. 24 (1990) 1275.
[3] D.H. Brown, H.R. Hitz, L. Schafer, Chemosphere 10 (1981) 245.

[4] R. Ganesh, G.D. Boardman, D. Michelson, Water Res. 28 (1994) 267.
[5] H.S. Lin, M.L. Chen, Water Res. 31 (1997) 868.
[6] J. Sarasa, M.P. Roche, M.P. Ormad, E. Gimeno, A. Puig, J.L. Olivelleiro, Water Res. 32 (1998) 2721.
[7] J. Wu, M.A. Eiteman, S.E. Law, J. Environ. Eng. 124 (1998) 272.
[8] F.M. Saunders, P.J. Gould, R.C. Southerland, Water Res. 17 (1983) 1407.
[9] J. Carriere, J.P. Jones, A.D. Broadbent, Ozone Sci. Eng. 15 (1993) 189.
[10] Y. Wang, Water Res. 34 (2000) 990.
[11] L.B. Reutergardh, M. Iangphasuk, Chemosphere 35 (1997) 585.
[12] F. Kiriakidou, D.I. Kondarides, X.E. Verykios, Catal. Today 54 (1999) 119.
[13] L. Szpyrkowicz, C. Juzzolino, S. Daniele, Ind. Eng. Chem. Res. 39 (2000) 3241.
[14] L. Szpyrkowicz, C. Juzzolino, S.N. Kaul, Water Res. 35 (2001) 2129.
[15] J. Naumczyk, L. Szpyrkowicz, G.F. Zilio, Water Sci. Technol. 11 (1996) 17.
[16] H.O. Finklea (Ed.), Semiconductor Electrodes, Elsevier, New York, 1988.
[17] K. Vinodgopal, D.E. Wynkoop, Environ. Sci. Technol. 30 (1996) 1660.
[18] R. Pelegrini, P.P. Zamora, A.R. Andrade, J. Reyes, N. Duran, Appl. Catal. B: Environ. 12 (1999) 83.
[19] J. Luo, M. Hepel, Electrochim. Acta 46 (2001) 2913.
[20] M.A. Anderson, M.J. Gieselmann, Q. Xu, J. Membr. Sci. 39 (1988) 243.
[21] L. Spanhel, M.A. Anderson, J. Am. Chem. Soc. 113 (1991) 2826.
[22] R.J. Candal, W.A. Zeltner, M.A. Anderson, J. Adv. Oxid. Technol. 3 (1998) 270.
[23] R.J. Candal, W.A. Zeltner, M.A. Anderson, J. Environ. Eng. 125 (1999) 906.
[24] R.J. Candal, W.A. Zeltner, M.A. Anderson, Environ. Sci. Technol. 34 (2000) 3443.
[25] Q. Xu, M.A. Anderson, J. Mater. Res. 6 (1991) 1073.
[26] J.J. Sene, W.A. Zeltner, M.A. Anderson, J. Phys. Chem. B, 2002, submitted for publication.
[27] D.H. Kim, M.A. Anderson, Environ. Sci. Technol. 28 (1994) 479.
[28] J.S. Do, W.C. Yeh, J. Appl. Electrochem. 25 (1995) 483.
[29] J.O. Callaway, in: L.S. Clesceri, A.E. Greenberg, R.R. Trussell, (Ed.), Standard Methods for the Examination of Water and Wastewater, 17th ed. APHA–AWWA–WPCF, Washington, 1989, part 4000, p, 62.
[30] B.P. Nelson, R. Candal, R.M. Corn, M.A. Anderson, Langmuir 16 (2000) 6094.